J|A|C|S
ARTICLES
Published on Web 05/31/2002

Homoleptic Tetrahydrometalate Anions MH_4^- (M = Sc, Y, La). Matrix Infrared Spectra and DFT Calculations

Xuefeng Wang and Lester Andrews*

Contribution from the Department of Chemistry, University of Virginia, Charlottesville, Virginia 22904-4319

Received January 22, 2002

Abstract: Laser-ablated Sc, Y, and La atoms react with molecular hydrogen upon condensation in excess argon, neon, and deuterium to produce the metal dihydride molecules and dihydrogen complexes MH_2 and $(H_2)MH_2$. The homoleptic tetrahydrometalate anions ScH_4^-, YH_4^-, and LaH_4^- are formed by electron capture and identified by isotopic substitution (D_2, HD, and $H_2 + D_2$ mixtures). Doping with CCl_4 to serve as an electron trap virtually eliminates the anion bands, and further supports the anion identifications. The observed vibrational frequencies are in agreement with the results of density functional theory calculations, which predict electron affinities in the 2.8−2.4 eV range for the $(H_2)ScH_2$, $(H_2)YH_2$, and $(H_2)LaH_2$ complexes, and indicate high stability for the MH_4^- (M = Sc, La, Y) anions and suggest the promise of synthesis on a larger scale for use as reducing agents.

Introduction

Homoleptic hydrometalate anions as anionic subunits are found in ternary solid-state materials containing hydrogen and transition, alkali or alkaline earth metals.[1] These materials have been intensively studied for many years because of efficient storage of hydrogen for commercial vehicular applications and hydrogenation in organic synthesis.[2−4] In addition, yttrium and lanthanum hydride films are known to undergo optical changes with hydrogen loading and to have applications as optical switches.[5]

Recent laser-ablation matrix-isolation experiments with palladium gave Pd atoms, which interact with H_2 to form the Pd-(H_2) complex; this complex captures an electron to give the linear isolated PdH_2^- molecular anion.[6] The analogous $(HPdH)^{2-}$ dianions surrounded by alkali metal cations have been recently characterized in solid materials.[7] In addition late first-row transition metal dihydride anions have been observed in the gas phase.[8] We wish to report matrix-isolation studies of Sc, Y, and La + H_2 systems, which produce dihydrogen complexes $(H_2)_xMH_2$ ($x = 1, 2$) and stable MH_4^- anions. Characterization of such species is relevant to understanding H_2 storage, optical switching devices, and hydrogenation in organic synthesis.

Experimental and Theoretical Methods

The experimental methods for reacting laser-ablated transition metal atoms with H_2 and identifying the reaction products with matrix infrared spectra have been described previously,[9−11] and the same methods were used here for the reaction of Sc, Y, and La with H_2. Laser-ablated metal atoms were co-deposited with 3−5% H_2 (or D_2, HD) in excess neon or argon and with pure deuterium onto a 3.5 K CsI window. Infrared spectra were recorded after deposition, annealing, and UV−vis irradiation. Several experiments were done with 0.1% CCl_4 added to 3% H_2 in neon or argon to serve as an electron trap,[10,11] and the absorptions due to anions were reduced markedly from the spectra of 3% H_2 samples.

Density functional theory (DFT) frequency calculations were performed to determine the structures and frequencies of new metal hydrides using the Gaussian 98 program.[12] The B3PW91 density functional and 6-311++G(d,p) basis set and SDD pseudopotential[13,14]

* Corresponding author. E-mail: lsa@virginia.edu.

(1) King, R. B. *Coord. Chem. Rev*. **2000**, *200*−*202*, 813 and references therein.
(2) Bronger, W. *Angew. Chem., Int. Ed. Engl.* **1991**, *30*, 759.
(3) Firman, T. K.; Landis, C. R. *J. Am. Chem. Soc.* **1998**, *120*, 12650.
(4) Chen, J.; Kuriyama, N.; Xu, Q.; Takeshita, H. T.; Sakai, T. *J. Phys. Chem. B* **2001**, *105*, 11214.
(5) Huiberts, J. N.; Griessen, R.; Rector, J. H.; Wijngaarden, R. J.; Dekker: J. P.; de Groat, D. G.; Koeman, N. J. *Nature* **1996**, *380*, 231.
(6) (a) Andrews, L.; Wang, X.; Alikhani, M. E.; Manceron, L. *J. Phys. Chem. A* **2001**, *105*, 3052. (b) Andrews, L.; Alikhani, M. E.; Manceron, L.; Wang, X. *J. Am. Chem. Soc*. **2001**, *122*, 11011.
(7) Olofsson-Martensson, M.; Haussermann, U.; Tomkinson, J.; Noreus, D. *J. Am. Chem. Soc.* **2000**, *122*, 6960 and reference therein.
(8) Miller, A. E. S.; Feigerle, C. S.; Lineberger, W. C. *J. Chem. Phys*. **1986**, *84*, 4127.
(9) Burkholder, T. R.; Andrews, L. *J. Chem. Phys*. **1991**, *95*, 8697.
(10) (a) (Sc + O_2): Chertihin, G. V.; Andrews, L.; Rosi, M.; Bauschlicher, C. W., Jr. *J. Phys. Chem. A* **1997**, *101*, 9085. (b) (Sc + O_2): Bauschlicher, C. W., Jr.; Zhou, M. F.; Andrews, L.; Johnson, J. R. T.; Panas, I.; Snis, A.; Roos, B. O. *J. Phys. Chem. A* **1999**, *103*, 5463. (c) (Y, La + O_2): Andrews, L.; Zhou, M. F.; Chertihin, G. V.; Bauschlicher, C. W., Jr. *J. Phys. Chem. A* **1999**, *103*, 6525.
(11) (a) Zhou, M. F.; Andrews, L. *J. Am. Chem. Soc.* **1998**, *120*, 11499. (b) Zhou, M. F.; Andrews, L. *J. Am. Chem. Soc*. **1999**, *121*, 9171.
(12) Frisch, M. J.; Trucks, G. W.; Schlegel, H. B.; Scuseria, G. E.; Robb, M. A.; Cheeseman, J. R.; Zakrzewski, V. G.; Montgomery, J. A., Jr.; Stratmann, R. E.; Burant, J. C.; Dapprich, S.; Millam, J. M.; Daniels, A. D.; Kudin, K. N.; Strain, M. C.; Farkas, O.; Tomasi, J.; Barone, V.; Cossi, M.; Cammi, R.; Mennucci, B.; Pomelli, C.; Adamo, C.; Clifford, S.; Ochterski, J.; Petersson, G. A.; Ayala, P. Y.; Cui, Q.; Morokuma, K.; Malick, D. K.; Rabuck, A. D.; Raghavachari, K.; Foresman, J. B.; Cioslowski, J.; Ortiz, J. V.; Stefanov, B. B.; Liu, G.; Liashenko, A.; Piskorz, P.; Komaromi, I.; Gomperts, R.; Martin, R. L.; Fox, D. J.; Keith, T.; Al-Laham, M. A.; Peng, C. Y.; Nanayakkara, A.; Gonzalez, C.; Challacombe, M.; Gill, P. M. W.; Johnson, B.; Chen, W.; Wong, M. W.; Andres, J. L.; Gonzalez, C.; Head-Gordon, M.; Replogle, E. S.; Pople, J. A. *Gaussian 98*, Revision A.6; Gaussian, Inc.: Pittsburgh, PA, 1998.
(13) (a) Becke, A. D. *J. Chem. Phys*. **1993**, *98*, 5648. (b) Perdew, J. P.; Wang, Y. *Phys. Rev. B* **1992**, *45*, 13244.
(14) (a) Frisch, M. J.; Pople, J. A.; Binkley, J. S. *J. Chem. Phys.* **1984**, *80*, 3265. (b) Andrae, D.; Haussermann, U.; Dolg, M.; Stoll, H.; Preuss, H. *Theor. Chim. Acta* **1990**, *77*, 123.

10.1021/ja020112l CCC: $22.00

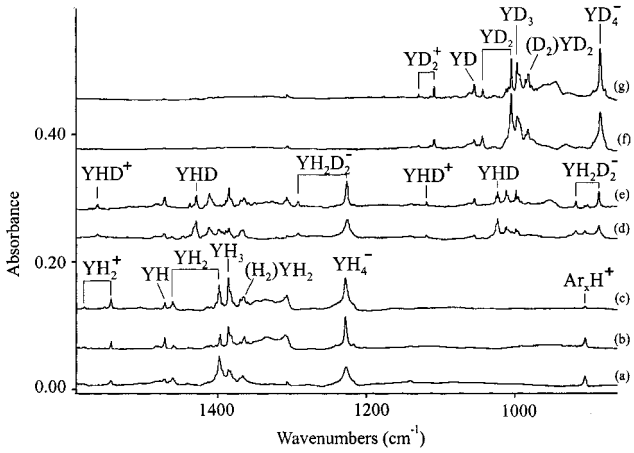

Figure 1. Infrared spectra in 1590−860 cm^{-1} region for laser-ablated yttrium co-deposited with argon/hydrogen samples: (a) 5% H_2 in argon deposited at 3.5 K for 60 min, (b) after annealing to 16 K, (c) after $\lambda >$ 240 nm photolysis for 15min, (d) 5% HD in argon deposited at 3.5 K for 70 min, (e) after annealing to 16 K, (f) 5% D_2 in argon deposited at 3.5 K for 60 min, and (g) after annealing to 16 K.

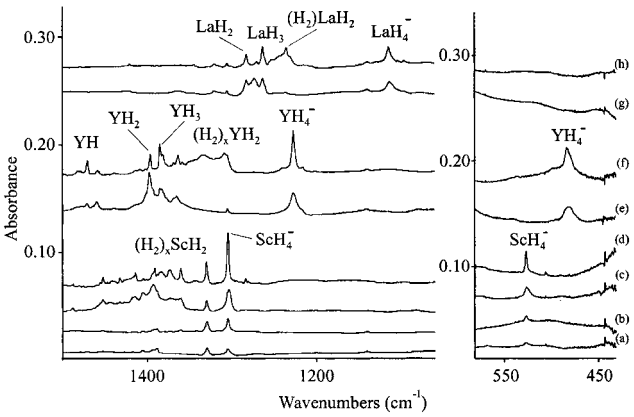

Figure 2. Infrared spectra in the 1500−1060 and 580−430 cm^{-1} regions for group 3 metal atom−hydrogen reaction products: (a) laser-ablated scandium co-deposited with 5% H_2 in argon at 3.5 K for 60 min, (b) after annealing to 16 K, (c) after $\lambda >$ 240 nm photolysis for 15 min, (d) after annealing to 25 K, (e) laser-ablated yttrium co-deposited with 5% H_2 in argon at 3.5 K for 60 min, (f) after annealing to 16 K, (g) laser-ablated lanthanum co-deposited with 5% H_2 in argon at 3.5 K for 60 min, and (h) after annealing to 16 K.

were employed, and the calculated frequencies were used to assign vibrational spectra. All geometrical parameters were fully optimized and the harmonic vibrational frequencies were obtained analytically at the optimized structures.

Results

Investigations into the reactions of laser-ablated Y, La, and Sc atoms with H_2 will be presented.

Y + H_2. Infrared spectra for the yttrium−hydrogen and yttrium−deuterium stretching regions are illustrated in Figure 1 for laser-ablated yttrium atoms co-deposited with H_2/Ar, HD/Ar, and D_2/Ar. The strong upper absorption at 1227.3 cm^{-1} tracks with a lower absorption at 482.7 cm^{-1}, which is compared in Figure 2. Annealing to 16 K sharpens and increases these spectral features and changes the relative intensities of several absorptions; broadband photolysis increases 1578.1, 1542.5, 1459.8, 1397.8, and 1385.1 cm^{-1} absorptions and slightly increases the integrated absorbances of the 1227.3 and 482.7 cm^{-1} bands, and further annealing to 20 K (not shown) increases the 1227.3 and 482.7 cm^{-1} bands by 30%. With D_2/Ar the upper band shifts to 882.3 cm^{-1} and the lower band shifts below our measurable region. The HD/Ar experiments gave three doublets: at 1291.4 and 1225.4 cm^{-1}, 915.7 and 884.5 cm^{-1} in the upper region and at 492.9 and 454.1 cm^{-1} in the lower region. The H_2 + D_2 experiments produced all of the above product bands. In solid neon similar bands were observed at 1233.3, 482.4 cm^{-1} with H_2, 887.9 cm^{-1} with D_2, and doublets at 1295.9 and 1232.4 cm^{-1}, 920.5 and 890.8 cm^{-1} with HD. A stronger D_2 counterpart band at 884.4 cm^{-1} was observed in pure solid deuterium. The observed frequencies are collected in Table 1. In addition, doping with CCl_4 eliminated the 1227.3 and 482.7 cm^{-1} bands in argon and the 1233.3 and 482.4 cm^{-1} bands in neon, which strongly suggests an anion identification.[10,11] The absorptions due to YH (1470.4 cm^{-1}), YH_2^+ (1578.1, 1542.5 cm^{-1}), YH_2 (1459.8, 1397.8 cm^{-1}), YH_3 (1385.1 cm^{-1}), and $(H_2)_xYH_2$ complexes (1363, 1337, 1309 cm^{-1}) will be discussed in detail in a later paper.

Table 1. Infrared Absorptions (cm^{-1}) for ScH_4^-, YH_4^-, and LaH_4^- in Excess Argon, Neon, and Deuterium at 3.5 K

	argon			neon			deuterium
	H_2	D_2	HD	H_2	D_2	HD	D_2
ScH_4^-			1377.0			1387.3	
	1305.1		1302.7	1321.3		1318.8	
			980.2			992.3	
		946.2	949.8		961.1	961.5	953.4
	527.1		523.5	527.6		526.6	
			494.2			497.1	
YH_4^-			1291.4			1295.9	
	1227.3		1225.4	1233.3		1232.4	
			915.7			890.8	
		882.3	884.5		887.9	920.5	884.4
	482.7		492.9	482.4			
			454.1				
LaH_4^-			1183.1			1158.5	
	1114.1		1112.4	1101.8		1096.3	
			833.5			825.0	
		797.8	799.8		788.7	788.8	783.2

La + H_2. Analogous experiments were done for laser-ablated lanthanum atom reactions with hydrogen in solid argon, neon, and pure deuterium. Infrared spectra for H_2 are shown in Figure 2 and the anion product absorptions are listed in Table 1. A new band appeared at 1114.1 cm^{-1} on deposition with H_2 in argon, increased 3-fold on broadband photolysis, and slightly increased on further annealing to 25 K. Deuterium counterparts appeared at 797.8 cm^{-1}, and HD and H_2 + D_2 experiments gave 1183.1, 1112.4, 833.5, and 799.8 cm^{-1} bands. The neon matrix spectra are very similar to argon matrix spectra; the 1101.8 cm^{-1} band with H_2 and the 788.7 cm^{-1} band with D_2 are the major product bands, and with HD four bands at 1158.5, 1096.3, 825.0, and 788.8 cm^{-1} were observed. A related band appeared at 783.2 cm^{-1} in pure deuterium. Unfortunately no bending mode is observed in our measurable lower region. A similar CCl_4 experiment for this system eliminated the 1114.1 cm^{-1} band. Again other species, LaH_3 (1263.6 cm^{-1}), LaH_2 (1320.9, 1283.0 cm^{-1}), $(H_2)LaH_2$ (1287.1, 1235.3 cm^{-1}), and higher hydrogen complexes were also trapped in the solid argon matrix.

Sc + H_2. Likewise, as shown in Figure 2, the strongest absorption at 1305.1 cm^{-1} in the reaction of Sc with H_2/Ar exhibits a lower 527.1 cm^{-1} component. The upper band shifts to 946.2 cm^{-1} with D_2/Ar. Similar isotopic absorptions with HD/Ar were observed at 1377.0 and 1302.7 cm^{-1}, 980.2 and 949.8 cm^{-1}, and 523.5 and 494.2 cm^{-1}. In addition the reactions in neon gave 1321.3, 527.6 cm^{-1} with H_2, 961.1 cm^{-1} with D_2,

Table 2. Calculated Vibrational Frequencies (cm^{-1}) and Intensities (km/mol) for Tetrahedral ScH_4^-, YH_4^-, and LaH_4^- Anions with T_d Symmetry[a]

ScH_4^-	ScD_4^-	$ScH_2D_2^-$
1456.2(a_1, 0)	1030.1(a_1, 0)	1389.4(462), 977.2(4730),
1305.5(t_2, 1219 × 3)	939.9(t_2, 638 × 3)	1304.1(1167), 942.8(708)
525.9(t_2, 434 × 3)	380.2(t_2, 203 × 3)	521.1(217), 488.4(349), 422.4(270), 374.2(93)
520.1(e, 0)	367.9(e, 0)	478.0(0)
YH_4^-	YD_4^-	$YH_2D_2^-$
1364.2 (a_1, 0)	965.0 (a_1, 0)	1309.0 (492), 919.7 (464)
1241.3 (t_2, 1255 × 3)	886.0 (t_2, 644 × 3)	1240.0 (1202), 888.3 (711)
502.0 (e, 0)	355.1 (e, 0)	434.4 (0)
476.4 (t_2, 516 × 3)	341.1 (t_2, 250 × 3)	489.2 (225), 444.4 (428), 379.9 (325), 347.7 (152)
LaH_4^-	LaD_4^-	$LaH_2D_2^-$
1234.0 (a_1, 0)	872.9 (a_1, 0)	1182.7 (578), 828.7 (547)
1118.9 (t_2, 578 × 3)	796.1 (t_2, 753 × 3)	1117.8 (1427), 798.2 (823)
474.8 (e, 0)	335.9 (e, 0)	411.2(0)
420.0 (t_2, 476 × 3)	299.5 (t_2, 233 × 3)	450.8 (173), 391.9 (395), 334.3 (301), 314.0 (175)

[a] Calculated at B3PW91/6-311++G(d,p)/SDD. Sc−H: 1.897 Å. Y−H: 2.063 Å. La−H: 2.232 Å.

and three pairs of bands at 1387.3 and 1318.8 cm^{-1}, 992.3 and 961.5 cm^{-1}, and 526.6 and 497.1 cm^{-1} with HD. Doping a 3% H_2/argon sample with 0.1% CCl_4 resulted in reduction of the 1305.1, 527.1 cm^{-1} bands to <20% of their absorbance in Figure 2a, and in contrast with Figure 2b−d, little growth was observed on annealing and photolysis. Finally, other scandium hydride species ScH (1530.4 cm^{-1}), and $(H_2)_xScH_2$ complexes were also trapped in the argon matrix.

DFT Calculations. DFT calculations were performed for ScH_4^-, YH_4^-, and LaH_4^- to determine the structures, frequencies, infrared intensities, and deuterium isotopic frequencies, which are listed in Table 2. All three anions have T_d symmetry with bond lengths of 1.897 (Sc−H), 2.063 (Y−H), and 2.232 Å (La−H), respectively.

Similar DFT calculations were done for the $(H_2)MH_2$ complexes, which converged with C_{2v} structures and gave real frequencies. The strongest MH_2 stretching modes are in excellent agreement with the bands observed and assigned here. The MH_2 stretching modes are 30−50 cm^{-1} lower in $(H_2)MH_2$ than in the isolated MH_2 molecules. The energy differences (MH_4^- minus $(H_2)MH_2$) provide electron affinities for $(H_2)MH_2$ and a prediction of stability for the MH_4^- anions. These energy differences are 2.79, 2.80, and 2.37 eV respectively for the Sc, Y, and La species. Similar calculations for AlH_4^- and (H_2)-AlH_2 yielded 2.97 eV, and the AlH_4^- anion is known to be stable.

Discussion

The yttrium, lanthanum, and scandium tetrahydrometalate anions will be identified based on isotopic substitution, comparison of argon, neon, and deuterium matrix spectra, and DFT frequency calculations.

YH_4^-. In solid argon the 1227.3 cm^{-1} band increased on annealing at the expense of $(H_2)YH_2$ complex absorption at 1363.4 cm^{-1}. Broadband photolysis increased YH_2 and (H_2)-YH_2 and slightly increased the 1227.3 cm^{-1} absorption. The deuterium counterpart band at 822.3 cm^{-1} showed the same annealing and photolysis behavior. The 1227.3 and 882.3 cm^{-1} bands can be assigned to antisymmetric Y−H and Y−D stretching fundamentals ν_3 (t_2) of the tetrahedral anions YH_4^- and YD_4^- on the basis of the following evidence. In the HD experiments the above bands split into 1291.4 and 1225.4 cm^{-1} and 915.7 and 884.5 cm^{-1} doublets, respectively, on symmetry lowering, which are due to symmetric and antisymmetric YH_2 and YD_2 stretching fundamentals in $YH_2D_2^-$. The antisymmetric YH_2 and YD_2 modes in $YH_2D_2^-$ are very close to the ν_3 (t_2) modes observed in YH_4^- and YD_4^-, respectively, and the new symmetric modes lie higher by about 64.1 cm^{-1} for the YH_2 mode and 33.4 cm^{-1} for the YD_2 mode in $YH_2D_2^-$ anion. This pattern of four Y−H(D) stretching modes for $YH_2D_2^-$ verifies a tetrahydride species as described for ZrH_4 and HfH_4.[15] Furthermore, the strong absorption at 482.7 cm^{-1} in argon, which splits to 492.9 and 454.1 cm^{-1} with HD, is due to the antisymmetric ν_4 (t_2) bending mode of YH_4^-. Finally, YH_2^+, YHD^+ and YD_2^+ (Figure 1) and the Ar_xH^+ and Ar_xD^+ species[16] are observed in these experiments, which provides for charge balance in the matrix.

In neon the Y−H and Y−D stretching modes in YH_4^- and YD_4^- appeared at 1233.3 and 887.9 cm^{-1}, respectively, and a similar four-band isotopic splitting pattern was observed for $YH_2D_2^-$. This is a typical blue shift for argon to neon matrices.[17] A strong 884.4 cm^{-1} band in pure deuterium, which is reduced on broadband photolysis and recovered partially on further annealing, is due to YD_4^-.

The strong degenerate ν_3 (t_2) mode computed for YH_4^- at 1241.3 cm^{-1} and YD_4^- at 886.0 cm^{-1} and the strong degenerate ν_4 (t_2) mode for YH_4^- at 476 cm^{-1} are in excellent agreement with observed values (Tables 1 and 2). For $YH_2D_2^-$ the calculated Y−H stretching splitting of 69.0 cm^{-1}, Y−D stretching splitting of 31.4 cm^{-1}, and Y−H_2 bending splitting of 44.8 cm^{-1} match very well with observed values of 66.0, 31.2, and 38.8 cm^{-1}, respectively.

The anion identification is further confirmed with CCl_4 additive, which serves as an electron trap agent. The elimination of YH_4^- with CCl_4 added to the sample shows that electron trapping is very effective in this system.[10,11] Hence, YH_4^- is identified here from the observation of four Y−H(D) stretching absorptions on HD substitution, agreement with DFT frequency calculations, and CCl_4 doping to verify the anion charge.

LaH_4^-. The analogous tetrahedral lanthanum hydride anion LaH_4^- was identified in the reaction of laser-ablated La atoms with molecular hydrogen in argon, neon, and pure deuterium matrix experiments, and the infrared absorptions are listed in Table 1. The La−H and La−D stretching modes observed at 1114.1 and 797.8 cm^{-1}, respectively, in argon exhibit tetrahydride HD substitution; both La−H and La−D stretching modes split into doublets at 1183.1, 1112.4 cm^{-1} and 833.5, 799.8 cm^{-1}. The neon matrix absorptions at 1101.8 and 788.7 cm^{-1} show the same isotopic distributions and confirm the tetrahydride assignment. However, in contrast to the blue matrix shift of YH_4^- for argon to neon, a red shift is observed for LaH_4^-. This is probably due to repulsive interaction and the tight fit of LaH_4^- into the more rigid argon matrix environment.

ScH_4^-. Assignment of 1305.1 and 527.1 cm^{-1} bands to the ν_3 and ν_4 modes of ScH_4^- follows from its similar chemical

(15) (a) Chertihin, G. V.; Andrews, L. *J. Am. Chem. Soc*. **1995**, *117*, 6402. (b) Chertihin, G. V.; Andrews, L. *J. Phys. Chem.* **1995**, *99*, 15004.
(16) Milligan, D. E.; Jacox, M. E. *J. Mol. Spectrosc.* **1973**, *46*, 460. Andrews, L.; Ault, B. S.; Grzybowski, J. M.; Allen, R. O. *J. Chem. Phys.* **1975**, *62*, 2461.
(17) Jacox, M. E. *Chem. Phys.* **1994**, *189*, 149.

and spectroscopic behavior to YH_4^- and LaH_4^-. Scandium atoms exhibit more thermal and photochemical reactions in low-temperature matrices, giving ScH_4^- as the dominant product after annealing and photolysis (Figure 2).

The ν_3 (t_2) mode for ScH_4^- is calculated slightly lower than the observed neon matrix value whereas these modes for YH_4^- and LaH_4^- are calculated slightly higher as is expected. Scandium is a more difficult calculation owing to competing low-lying atomic configurations.[18]

Comparisons. Note that in argon the Sc−H and La−H stretching modes lie 77.8 cm^{-1} higher and 113.2 cm^{-1} lower, respectively, than the Y−H stretching mode. The bending mode for ScH_4^- appeared at 527.1 cm^{-1}, and for YH_4^- at 482.7 cm^{-1}, and we can infer that this mode for LaH_4^- is below 400 cm^{-1}, which is out of our measurable region. The antisymmetric M−H stretching mode ν_3 (t_2) decreases from 1305.1 cm^{-1} for ScH_4^- to 1227.3 cm^{-1} for YH_4^- and to 1114.1 cm^{-1} for LaH_4^-, suggesting a straightforward metal−hydrogen bond length increase from ScH_4^- to YH_4^- and to LaH_4^-, respectively, which is in line with our DFT computations.

The isoelectronic TiH_4, ZrH_4, and HfH_4 molecules exhibit ν_3 (t_2) modes at 1663.8, 1623.6, and 1678.4 cm^{-1}, respectively, in solid argon.[15,19,20] The increase in frequency from ZrH_4 to HfH_4 has been attributed to the relativistic bond-length contraction predicted for HfH_4 (1.907 Å) relative to ZrH_4 (1.912 Å).[21,22] However, La and Hf are separated by the 14 elements of the lanthanide series, and no such contraction occurs for La relative to Y as is shown here.

Here electron affinity plays an important role in the formation of the metal tetrahydrometalate anions. The electron affinities predicted from DFT, 2.79 eV for $(H_2)ScH_2$, 2.80 eV for $(H_2)YH_2$, and 2.37 eV for $(H_2)LaH_2$, are substantial and only slightly lower than the 2.97 eV value calculated for $(H_2)AlH_2$ at the same level of theory. The stable isolated AlH_4^- anion in an argon matrix is attested by its formation through UV irradiation (240 nm) of aluminum samples containing the $(H_2)AlH_2$ complex.[23] Similar laser-ablation experiments give isolated AlH_4^- at 1609.0 cm^{-1} in solid argon, which is in excellent agreement with the matrix photolysis experiments.

A final comparison between electron detachment energies predicted here for ScH_4^- and YH_4^- (2.79 and 2.80 eV, respectively) and those for ScO_2^- and YO_2^- can be made. The latter have been measured as 2.32 and 2.00 eV, respectively,[24] and computed as 2.4 and 1.9 eV, respectively.[10] In similar investigations of the reactions of laser-ablated Sc, Y, and La atoms with O_2, the stable MO_2^- anions were observed as the major products; although the MO_2^- absorptions increased slightly on annealing to 20−25 K, they were destroyed on full-arc photolysis.[10] In contrast, the MH_4^- ions increased on full-arc photolysis. Hence, the tetrahydrometalate anions of Sc, Y, and La are more stable than their dioxide anions.

Reaction Mechanisms. Laser-ablated metal atoms react with hydrogen molecules to give the MH_2 (M = Sc, Y, La) dihydride molecules, and the $(H_2)MH_2$ complexes are formed spontaneously instead of tetrahydrides on the association of another H_2 reagent because of the trivalent state of this metal group. However, electrons are abundant in the ablation plume and $(H_2)MH_2$ can capture an electron to provide four valence electrons and form the tetravalent anion. The spectra in Figures 1 and 2 summarize this process. The YH_2 molecule complexes one or two dihydrogen molecules on annealing to allow diffusion of reagents (Figure 1, absorptions in the 1370−1300 cm^{-1} region). The MH_4^- anion absorptions increased on annealing and broadband photolysis, which indicates the strong attraction for electrons in this stable species. Furthermore, the same $MH_2D_2^-$ anion is prepared from HD and $H_2 + D_2$ mixtures, which shows that the anion is homoleptic; however, the MHD product is spectroscopically distinct from MH_2 and MD_2.

$$M + H_2 \rightarrow MH_2 \quad (1)$$

$$MH_2 + H_2 \rightarrow (H_2)MH_2 \quad (2)$$

$$(H_2)MH_2 + e \rightarrow MH_4^- \quad (3)$$

During the deposition process, electrons from laser ablation of the target surface are captured in reaction 3 to form MH_4^- anions; hence, the addition of CCl_4 minimizes the MH_4^- yield by preferential capture of these ablated electrons.[11] Photolysis of the prepared samples increases the MH_4^- anion yield (ScH_4^- and LaH_4^- more than YH_4^-); this suggests that electrons from photodetachment of a less stable anion in the matrix allow the formation of the more stable MH_4^- anions. In the La case the ionization energy is sufficiently low (295 nm) for La atoms to serve as a photoelectron source. Finally, the pronounced growth of MH_4^- absorptions on annealing to 16−25 K is unusual as ions are reactive, and higher annealing to 30−40 K markedly decreases the MH_4^- absorptions. How then do the MH_4^- anions increase on early annealing? The most likely additional trapping site for ablated electrons in these experiments is as the hydride anion, H^- (the electron affinity of atomic hydrogen is 0.76 eV).[25] The small H^- ion should diffuse in the matrix and electron transfer to species with higher electron affinities such as the $(H_2)MH_2$ complexes.

Conclusions

Matrix-isolation experiments and DFT calculations show that Sc, Y, and La atoms energized by laser ablation react with molecular hydrogen to form dihydrides and higher dihydrogen complexes. Electron capture leads to stable Sc, Y, and La tetrahydrometalate anions, which are isoelectronic with AlH_4^-. Doping with CCl_4 to serve as an electron trap almost eliminates the anion absorptions and attests to the anion identification. DFT calculations predict frequencies in agreement with the matrix observations and electron affinities in the 2.4−2.8 eV range for the $(H_2)MH_2$ complexes that form the stable MH_4^- anions. The group 3 tetrahydride anions should be sufficiently stable for synthesis on a larger scale and use as reducing agents.

Acknowledgment. We gratefully acknowledge support for this work from N.S.F Grant CHE 00-78836

JA020112L

(18) Bauschlicher, C. W., Jr.; Langhoff, S. R. *J. Chem. Phys.* **1986**, *85*, 5936.
(19) Xiao, Z. L.; Hague, R. H.; Margrave, J. L. *J. Phys. Chem.* **1991**, *95*, 2696.
(20) Chertihin, G. V.; Andrews, L. *J. Am. Chem. Soc.* **1994**, *116*, 8322.
(21) Pyykko, P.; Snijders, J. G.; Baerends, E. J. *Chem. Phys. Lett.* **1981**, *83*, 432.
(22) Pyykko, P. *Chem. Rev.* **1988**, *88*, 563.
(23) Pullumbi, P.; Bouteiller, Y.; Manceron, L. *J. Chem. Phys.* **1994**, *101*, 3610.
(24) Wu, H.; Wang, L.-S. *J. Phys. Chem. A* **1998**, *102*, 9129.
(25) Berry, R. S. *Chem. Rev.* **1969**, *69*, 533.